Arabian Journal of Geosciences (2020) 13: 644
https://doi.org/10.1007/s12517-020-05606-1

ORIGINAL PAPER

Varying characteristics of electromagnetic radiation from coal failure during hydraulic flushing in coal seam

Hao Wang [1,2] · Wang Enyuan [1,2] · Zhonghui Li [1,2] · Xiaoran Wang [1,2] · Dexing Li [1,2] · Muhammad Ali [1,2,3] · Qiming Zhang [1,2]

Received: 23 August 2019 / Accepted: 22 June 2020 / Published online: 11 July 2020

Abstract

A large amount of gas, which will do great damage to the environment as a kind of greenhouse gas, is discharged directly into the air in the process of coal mining in China. Majority of coal mines in China are characterized by low permeability, great gas pressure, and low strength feature. These features make it difficult for the extraction of gas, which increases the risk of coal and gas outbursts. In order to improve the permeability of coal seam, hydraulic flushing (HF) technology is adopted. So, the effect of hydraulic flushing will be necessary to be analyzed before gas extraction. In this paper, an electromagnetic radiation (EMR) experiment system of coal seam during hydraulic flushing was established, electromagnetic radiation (EMR) signals produced by the deformation and fracture of coal were studied during hydraulic flushing in coal seam in the Songhe coal mine, Guizhou province, China. The results showed that abundant EMR signals could be produced because of coal deformation and fracture. EMR signals were positively associated with the degree of coal failure. In different coal seams, EMR signals had different features during hydraulic flushing. The greater the gas pressure in the coal seam, the more dilatation energy was released. Higher rupture velocity could generate stronger magnetic signals. During hydraulic flushing, the more serious the rupture of coal, the higher the count of EMR pulses, and the higher the frequency of EMR. The principal frequencies and the amplitudes of waves increased gradually with gradually increasing ruptures. The change of EMR signals after hydraulic flushing was more dramatic than before hydraulic flushing. So, it is feasible and dependable to evaluate the effect of coal seam hydraulic flushing by EMR.

Keywords Gas · Coal seam · Hydraulic flushing · Deformation and fracture · Electromagnetic radiation

Responsible Editor: Zeynal Abiddin Erguler

Electronic supplementary material The online version of this article (https://doi.org/10.1007/s12517-020-05606-1) contains supplementary material, which is available to authorized users.

✉ Wang Enyuan
weycumt@cumt.edu.cn

Hao Wang
whcumt@cumt.edu.cn

Zhonghui Li
76371524@qq.com

Xiaoran Wang
1941286070@qq.com

Dexing Li
179785183@qq.com

Muhammad Ali
ali.uet@icloud.com

Qiming Zhang
qimingzhang@cumt.edu.cn

[1] Ministry of Education, Key Laboratory of Gas and Fire Control for Coal Mines, China University of Mining and Technology, Xuzhou 221008, Jiangsu, China

[2] School of Safety Engineering, China University of Mining and Technology, Xuzhou 221008, Jiangsu, China

[3] Department of Mining Engineering, Engineering & Management Sciences, Balochistan University of Information Technology, Quetta, Pakistan

Introduction

Coal and gas outbursts are among the most serious mine disasters in China. When an outburst occurs, huge amounts of coal and gas are ejected from the working face in an instant, which cannot only destroy mining infrastructure like roadways and ventilation systems but also cause asphyxiation and burial deaths, and even gas or coal-dust explosions and so on (Wang et al. 2012a, b; Xie et al. 2015; Cao et al. 2018; Shen et al. 2018; Gonzatti et al. 2014). In recent years, with increased depth and intensity of coal mining, the coupling effect of high stress and great gas pressure has been enhanced. Such coupling can affect the gestation, occurrence, and development processes of a disaster to complicate the destructive mechanism and cause a "composite effect" (Pan 2016; Liu et al. 2017), decreasing the "thresholds of prerequisite" for dynamic disasters and increasing the risk of coal and gas outbursts (Zhou et al. 2016). Gas disasters have become a serious issue, restricting the safe and efficient production of coal mines in China. Gas pre-drainage is the most important measure to prevent gas disasters during mining of high gas content coal seams, which helps ensure safe production. Gas predrainage not only decreases the gas pressure of a coal seam to reduce the risk of coal and gas outbursts, but it also reduces the degree of coupling and improves the mechanical properties of coal to decrease the likelihood of compound disasters(Wang et al. 2012a, b, 2014; Bamberger et al. 2014). Therefore, the efficiency of gas extraction directly affects the prevention and control of coal and gas outbursts. However, coal seam structures in China are complex; for instance, most coal seams have the characteristics of high ground stress, microporosity, low permeability, and high absorptivity, resulting in poor gas extraction and difficult-to-control gas movement (Liu and Cheng 2015). To solve these problems, traditional methods such as reducing the distance between boreholes, increasing the borehole diameter, increasing the number of boreholes, and prolonging gas extraction time, have been conducted. However, extraction results were not satisfactory, and gas levels exceed the standard limits during coal mining, which causes huge security risks. Therefore, new methods of gas extraction and gas control are required.

The coupled effects of ground stress, gas pressure, mechanical properties of the coal mass, and geologic structure are generally believed to cause coal and gas outbursts (Geng et al. 2017). Coal seams with low permeability, high gas pressure, soft coal, and low strength near the ground stress zone and geologic structure zone are prone to coal and gas outbursts. After in-depth study of mechanism, law, and control methods of coal and gas outbursts, a series of precautionary measures and evaluation systems have been used in China. Deep hole blasting, coal seam affusion, hydraulic fracture, hydraulic slotting, and other technologies are used to reduce the risk of coal and gas outburst. But these technologies have certain limitations, such as the process of deep hole blasting cannot be manually controlled; The influence scope of coal seam affusion is small. Hydraulic fracture tends to produce a large stress concentration area and induce coal and gas outburst. Hydraulic slotting requires a good proppant to support the fracture. Hydraulic flushing (HF) is one of the more mature and widely applied technologies to reduce risks of outbursts. HF uses rock or coal roadways as a safety barrier, with a high-pressure water jet from the drill nozzle to break the coal mass in the coal seam. Part of the gas and the broken coal mass are ejected along the drill way, and a hole is formed in the coal seam; then the coal mass near the hole swells and distorts, causing displacement under the effect of ground stress. A large number of cracks are generated to unload ground stress, increase the permeability, and improve gas extraction in a shorter time. Therefore, HF not only reduces outburst risk but also changes the mechanical characteristics of outburst coal seams, which makes HF widely applicable to prevent coal and gas outbursts in coal mining (Liu 2009; Yang and Wang 2010). It is necessary to evaluate the effect of pressure relief and permeability enhancement to ensure the gas extraction rate reaches the standard (Kong et al. 2016a, b). A number of traditional methods, such as measuring the residual gas and water content of coal, and inspecting changes in parameters of gas extraction, have been adopted to evaluate the effect of HF. However, these traditional methods all emphasized the aspect of gas extraction after HF. The effect of coal failure during HF, which directly affects gas extraction, lacks sufficient research. If the effects of coal failure can be dynamically monitored during HF, it will provide guidance for the pre-evaluation of gas extraction.

HF uses a high-pressure water jet to break the coal mass, which releases energy when it fractures. Electromagnetic radiation (EMR), which is one kind of energy produced when coal and rock ruptures, is positively associated with the degree of coal failure (He et al. 2010). EMR signals will be stronger when the fracture of coal and rock is more serious. An electrical parameter test system of loaded coal and rock was established to study the EMR effect in different deformation and fracture processes of coal and rock (Wang et al. 2011; Song et al. 2015). The mechanism of EMR signal generation during coal and rock deformation and fracture is complicated. Many scholars have proposed various theories, such as the accelerated motion of charges at the crack tip, piezoelectric effect, friction charging, or the oscillation and transience of the electric dipole (Nitsan 1977; Chishko and Charkina 1997). The EMR signal generated by deformation and fracture of coal and rock is the result of comprehensive effects of these micro-mechanisms. The correlation between the loading of coal and rock and the EMR signal has been studied. A large number of research results showed that the more serious the coal and rock fracture, the stronger the EMR(Song et al. 2016; Qiu et al. 2017).So, EMR signals can be used as precursory

information of coal and rock fracture(He et al. 2012; Wang and Zhao 2013; Kong et al. 2016a, b).Based on the above research results, EMR technology has been applied widely to monitor internal stability of coal or rock and predict dynamic disasters, which has led to better field applications (Frid 1997; Lichtenberger 2006; He et al. 2011).

As a new technology for reducing outbursts, HF is being popularized in the coal mine industry. EMR technology has also been applied widely because of its superior performance in monitoring and predicting coal and rock dynamic disasters, providing early warnings. Therefore, real-time and dynamic monitoring of the degree of coal failure by combining the highly sensitive EMR technology was of great significance during HF (Shen et al. 2019, 2018). During HF, the process of the fracture of coal can be obtained by analyzing the varying characteristics of EMR signals. Based on this, this paper presents monitoring and analysis results for EMR intensities and pulses produced by the deformation and fracture of coal during HF in different coal seams. The #17 and #18 coal seams in the Songhe coal mine, Guizhou province, China, which are characterized by low permeability, great gas pressure, and low strength feature, used as a case study. The results have guiding significance in the application of EMR to evaluate the effect of HF.

Geological background

The Songhe coal mine is in the southeastern Panxian county coal field, in southwestern Guizhou province. It is located in the middle section of the north limb of the Tucheng synclines, in Songhe township, Liupanshui city (Fig. 1). The field is oriented north 60° west, extending southwest. The highest elevation is + 2301.66 m above sea level (asl), and the lowest elevation is + 1629.23 m asl. The annual production of the Songhe coal mine is 2.4 million tons. The absolute gas emission rate of the coal mine was more than 140 m^3/min in 2004 and a serious gas outburst has occurred in the mine, so the mine is considered as high gas outburst mine.

The Songhe mine contains 18 layers of primary mineable and partially mineable coal seams, and the main coal seams are at risk of coal and gas outbursts. According to existing data for coal seams, the #17 and #18 coal seams, with thicknesses of 3 m and 2 m, dip angles of approximately 20 to 32°, and depths of 550 m to 600 m, are 3.4 m apart in the west limb of the second mining area. The maximum gas pressure and gas content of the #17 coal seam are 2.4 MPa and 14 m^3/t, respectively, and the Protodyakonov coefficient is 0.44. The maximum gas pressure and gas content of the #18 coal seam are 2.5 MPa and 14.73 m^3/t, respectively, and the Protodyakonov coefficient is 0.36. The permeability coefficient of the #17 and #18 coal seams is 0.26 m^2/MPa^2 day for both. All the data show that these coal seams are characterized by high stress, high gas pressure, low permeability, and low mechanical strength and, thus, the phenomenon of sudden gas emission is a regular occurrence when the cross-boreholes are being drilled in the ceiling of a rock roadway. It is evident that the gas in #17 and #18 coal seams is difficult to extract, and has a considerable risk of outburst.

To prevent coal and gas outbursts during mining, HF is adopted in the mine as a measure of gas control and to improve gas extraction efficiency. Cross-boreholes are drilled in the 12,171 floor drainage roadway, which is a rock tunnel excavated in the #17 coal floor. Then, HF is adopted in #17 and #18 coal seams. Figure 1 shows the location of hydraulic flushing.

Main components of HF and EMR signal monitoring system

Main components of HF

The HF system consists of five parts (Fig. 2): (1) Emulsification pump, which provides high pressure; (2) Hydraulic control valve, which changes the water pressure according to HF needs; (3) Water tube, which transports high-pressure water; (4) Drilling rig, which provides power to drill in the coal seams; (5) Other equipment, including a rotator which connects the water tube and drilling rig, a drill bit, some ejectors installed in the drill bit for flushing, and some drill pipes that connect the drill bit and rotator to transport high-pressure water.

EMR signal monitoring system

To further study coal failure during hydraulic flushing in different coal seams and evaluate the effects of hydraulic flushing, an EMR monitoring instrument, YDD16, developed by the University of Mining and Technology of China to predict coal and rock dynamic disasters, is applied during hydraulic flushing. The system consists of a high-sensitivity antenna which can receive directional signals in a range from 7 to 22 m, and a processor that can analyze EMR signals received by the high-sensitivity antenna to show pulses, energy, average intensity, time, and so on. Figure 2 shows the components and monitoring principles of the YDD16.

Field experiment

The main procedures

1. Drill a borehole with designated length and angle across the #17 and #18 coal seams in the HF location (Fig. 3).

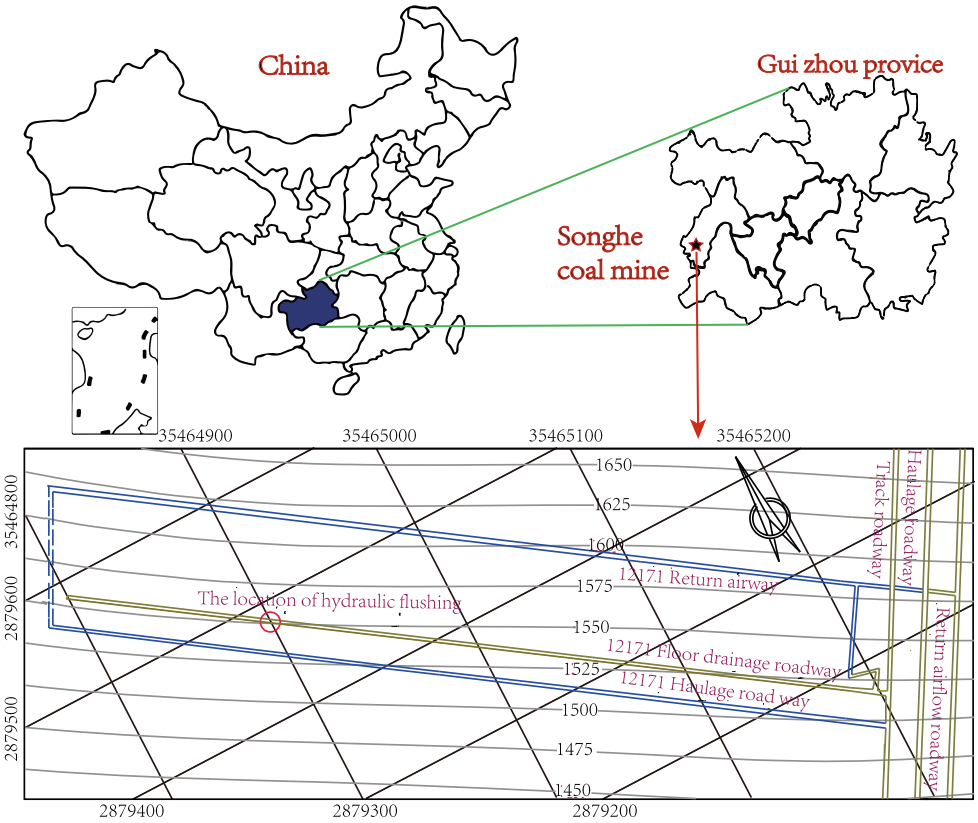

Fig. 1 Location of the Songhe coal mine and location of hydraulic flushing

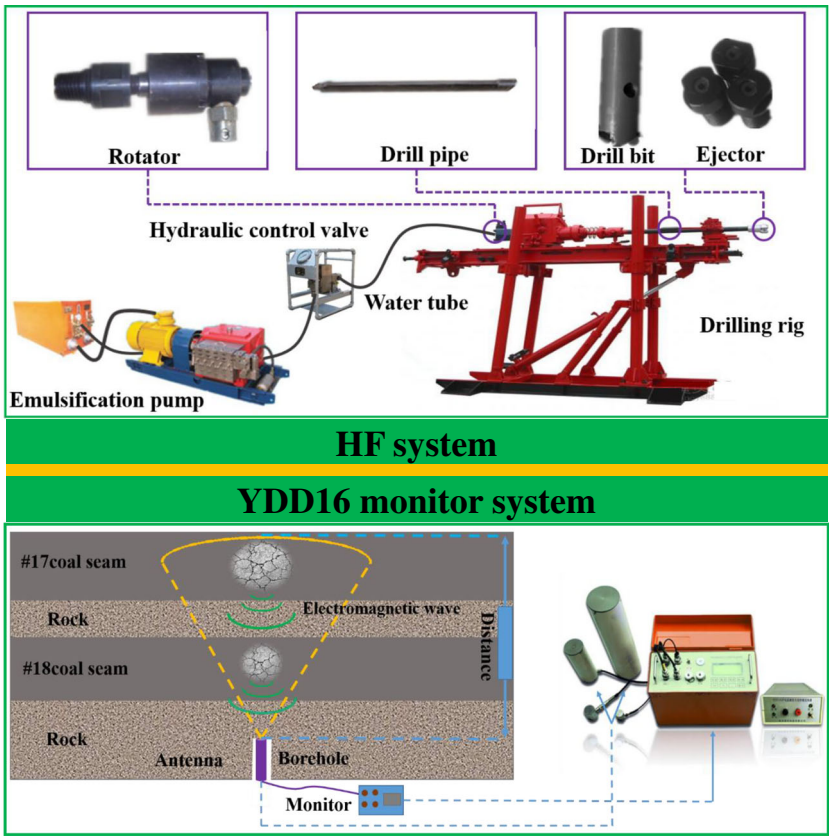

Fig. 2 Components of the HF system and YDD16 monitor system

2. Drill another borehole 1 m from the last borehole with the same length and angle, in which the YDD16 antenna is placed to monitor EMR signals.
3. Start the emulsifying pump to deliver high-pressure water. During HF, the drill pipe continues to revolve at a low constant speed, which is conducive to the discharge of coal mass along with water through the borehole.
4. HF continued for 2 h, so that first the #17 coal seam is flushed for 1 h and then the #18 coal seam is flushed. The YDD16 is battery powered. To avoid battery power loss during long-term monitoring, specific time points were chosen to monitor EMR signals for 300 s at a time. These points were before the start of HF; 5 min, half an hour, and 1 h after HF begins in each coal seam; and 24 h after the end of HF.

Results of EMR signal testing

EMR signal monitoring

As shown in Fig. 4 and Appendix A1–A7, before the start of HF, the various indexes of EMR signals are low. Beyond interference signals from the environment, there are no EMR signals from the fracture of coal. HF is conducted in #17 coal seam, first. Five minutes after HF starts, EMR signal strength begins to increase, indicating the increase of EMR pulses and energy. As time goes on, the signal gets stronger and stronger. There is a drop in signal strength at the 50-s mark in the monitoring period because of the instability of water pressure, which influences the rate of coal failure. Half an hour after HF starts, the EMR pulses and energy are at a higher level compared with the EMR signals of the initial stage of HF, demonstrating that coal fracture strength is increasing. The attenuation of EMR signals begins around the 100 s mark in the monitoring period. When HF has been carried out for an hour, the hole in the coal seam is so big that the pressure of the water jet cannot break up the coal effectively and continually. So, HF in the #17 coal seam finishes, and can begin in the #18 coal seam.

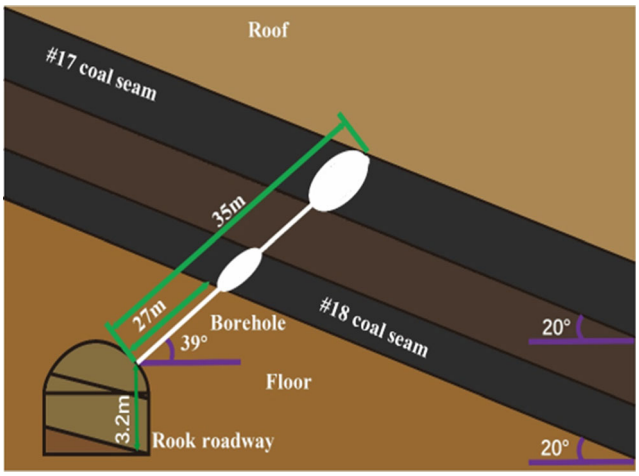

Fig. 3 Schematic diagram of borehole layout of HF

The EMR signals are stronger in the #18 coal seam than those in the #17 coal seam 5 min after HF begins. When HF has been proceeding for half an hour in the #18 coal seam, the changes of EMR pulses and energy are consistent with those in the #17 coal seam. The values are higher than those in the #17 coal seam because of the higher gas content. During HF monitoring at one and a half hours in the #18 coal seam, gas inrush occurs at 65 s and 267 s marks, where a mass of water, coal and gas erupted in an instant. The EMR signal intensities reflect these events. Furthermore, the quantities of water, coal, and gas erupted during the second gas inrush were even greater than the first time, indicating a more intense rupture.

It is important to avoid forming a very large hole in the coal seam, which may cause the problems during mining. Additionally, when the hole is large enough, the jet flow is not sufficient to break coal, so HF cannot be conducted. When the EMR signals begin to decrease 2 h after the start of HF, indicating decreasing rupture of coal, HF must be stopped.

Twenty-four hours after the end of HF, the EMR signal strengths have fallen sharply compared with the intense rupture of coal during HF. However, because of coal creep, the intensity of EMR signals is higher than that before the start of HF.

When HF is conducted over time or in different coal seams, the EMR pulses and energy are different. To understand the differences, the EMR pulses energy of the eight periods were averaged. Figure 5 shows that in both the #17 and the #18 coal seam, the average EMR pulses and energy first increase and then decrease. The averages in each period of HF for the #18 coal seam are higher than those in the #17 coal seam.

Changes in EMR energy

Figure 6 shows the EMR energy distributions for different monitoring time periods. The higher the EMR energy, the stronger the fracturing. EMR energy can be used to analyze the rupturing of coal during HF. The EMR energy increases with increasing time at the beginning. In the middle of the HF process, EMR energy maintains high levels. Later, it began to decrease. It is clear that the EMR energy during HF in the #18 coal seam is higher than that in the #17 coal seam. The changes in EMR energy seem to be in the shape of a parabola.

Changes in EMR pulse counts

In different coal seams and time periods, EMR pulses reflect the rupture of coal. For instance, the higher the count of EMR pulses, the more serious the rupture of coal, and the lower the count of EMR pulses, the less serious the rupture. Figure 7 and

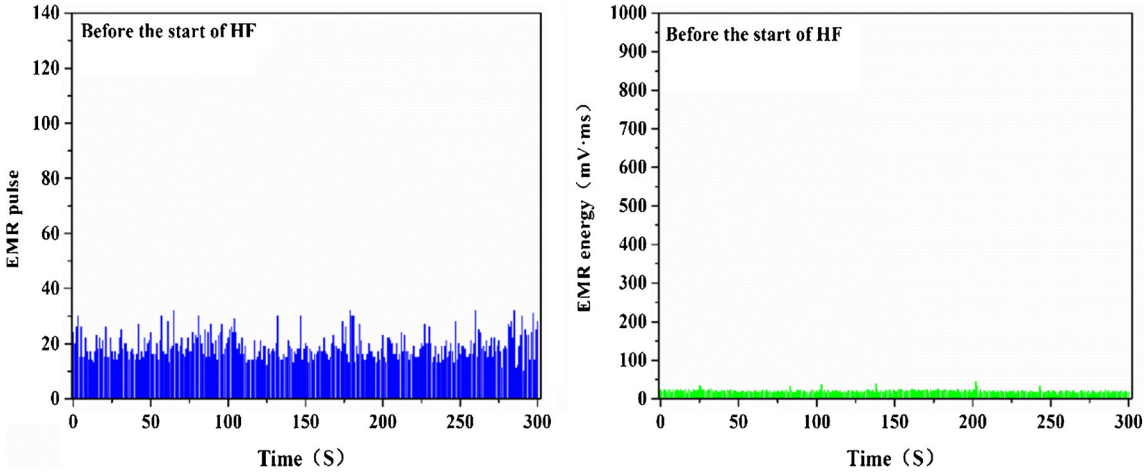

Fig. 4 The variation rule of EMR signals before the start of HF

Appendix B1–B3 show that lower EMR pulses mainly occur in the initial period of HF. Then, higher EMR pulses become more frequent, meaning that ruptures become more serious over time. When HF is over in the #17 coal seam or in the #18 coal seam, the high EMR pulses decrease and low EMR pulses begin to dominate. During HF, the numbers of high EMR pulses in the #18 coal seam are more than those in the #17 coal seam, indicating that the degree of fracturing is more severe. From the counts of EMR pulses after HF, it is seen that fracturing continues but is not serious.

Characteristics of frequency spectra of EMR signals

There is a lot of information about coal fracturing in EMR waveforms. To analyze EMR waveforms, the frequency spectra can be obtained by converting from the time domain to the frequency domain by fast Fourier transform (FFT). Figure 8 and Appendix C1, C2 show frequency spectra of EMR signals during HF in the #17 coal seam. Frequency zones are different in different time periods of HF. During HF, the frequency zones increase first and then decrease, which is related to the rupture of coal. Low principal frequencies are generated by microfractures. Serious fractures cause high principal frequencies. The wave amplitudes follow the same rules, proving that the principal frequency is positively associated with coal failure.

Discussion

A coal mass can be deformed and ruptured by loading from overburden stress and impacts of high-pressure water jets, as in HF. The process of fracture and deformation is a complete physical and chemical process. In this process, the piezoelectric effect and triboelectrification can take place because of charged defects in the coal mass, the rupture of covalent

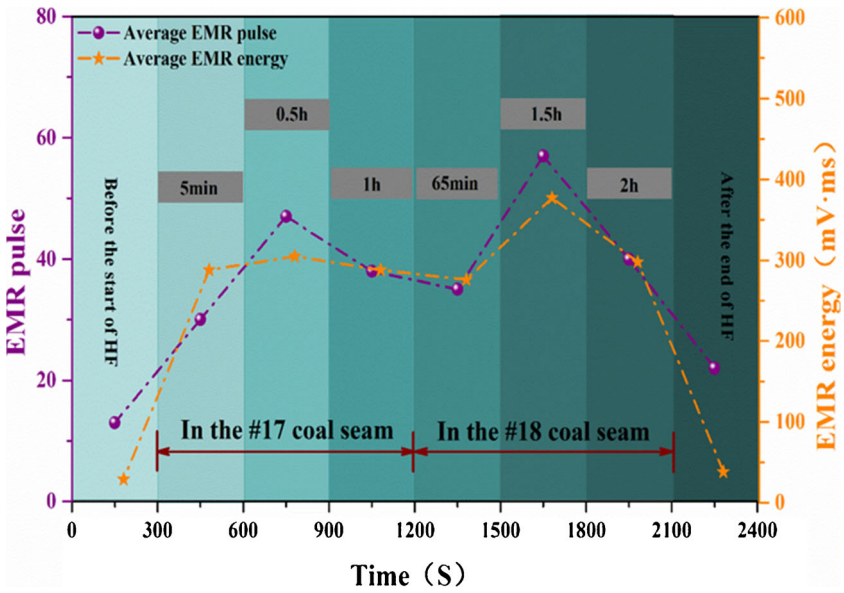

Fig. 5 Average EMR pulses and energy for HF at different times

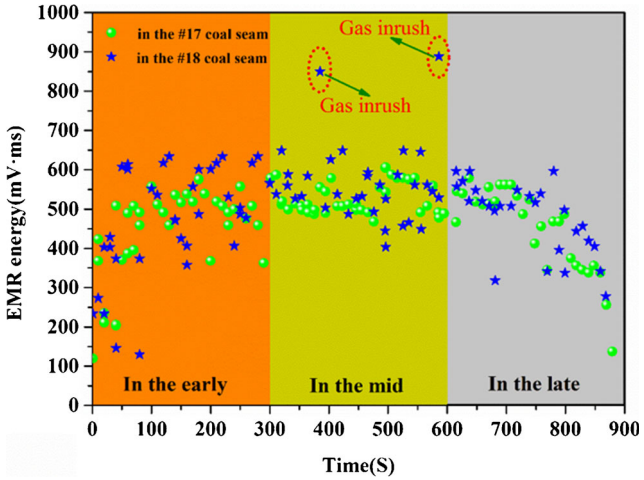

Fig. 6 Accumulated EMR pulses of hydraulic flushing (HF) at different times

bonds, and changes in intermolecular forces (Nitsan 1977). The free charges migrate and spread from the micro-crack walls and large amounts of dipoles form, which emit electromagnetic waves (Lou et al. 2019; Nie et al. 2009). EMR is therefore associated with the fracture and deformation of coal. Before the start of HF, there is no EMR signal generated by the fracture of coal because of mechanism equilibrium, but there are interference signals from the environment, which is why EMR signals are not zero. Once HF starts, fracture and deformation of coal occurs, which produces EMR signals. Changes in these EMR signals were analyzed.

The varying characteristics of EMR

According to the electric coupling model of deformation and failure of coal and rock (Kong et al. 2017), the relationship between EMR pulses and coal stress-strain is shown as:

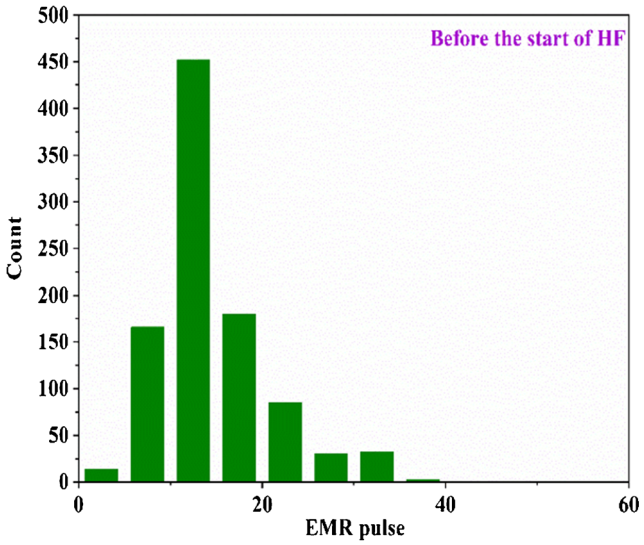

Fig. 7 Changes in EMR pulse counts before the start of HF

$$\frac{\sum N}{N_m} = 1-\exp\left[\left(\frac{\varepsilon}{\varepsilon_0}\right)^m\right] \quad (1)$$

where $\sum N$ is the cumulative number of EMR pulses and N_m is the cumulative number of EMR pulses in the area of S_m for the total rupture. There is a relationship between the damage parameter D(ε) and EMR pulses:

$$\mathrm{D}(\varepsilon) = \frac{\sum N}{N_m} \quad (2)$$

From eqs. (1) and (2), we obtain:

$$\sum N = D(\varepsilon)N_m \quad (3)$$

As seen in Fig. 9, a coal mass on the internal surface of an ordinary borehole is subjected to yield under the action of the drill bit, and the internal stress of the coal mass unloads. Thus, the coal mass in the II and III regions exhibits initial damage D_{ori}, and the coal mass in the IV and V regions does not exhibit initial damage. When the coal mass is completely broken, the damage to the coal mass in the II and III regions, caused by the high-pressure water jet, is 1-D_{ori}; and the damage to the coal mass in the IV and V regions, caused by the high-pressure water jet, is 1. According to Eq. (3), the EMR pulse generated by the fracture of coal in the II and III regions is:

$$\mathrm{N}_1 = D(\varepsilon)N_m = (1-D_{ori})N_m \quad (4)$$

and the EMR pulse generated by the fracture of coal in the **IV** and **V** regions is:

$$\mathrm{N}_2 = D(\varepsilon)N_m = N_m \quad (5)$$

From Eqs. (4) and (5), the following conclusion can be obtained:

$$\mathrm{N}_1 < \mathrm{N}_2 \quad (6)$$

Therefore, in the early stages of HF, when the high-pressure water jet impacts the coal bodies in regions II and III, the coal bodies broke up easily and produced small EMR signals.

During HF, the coal mass near the drill bit is first broken by the high-pressure water jet, and the area of the failure surface is S_1 (Fig. 10). Then, the coal mass away from the drill bit is broken by the high-pressure water jet, and the area of the failure surface is S_2. It is obvious that:

$$S_1 < S_2 \quad (7)$$

It is hypothesized that the EMR pulse generated by the fracture of coal in a unit area is N_0. The EMR pulse generated by the fracture of coal mass in S_1 is N_l:

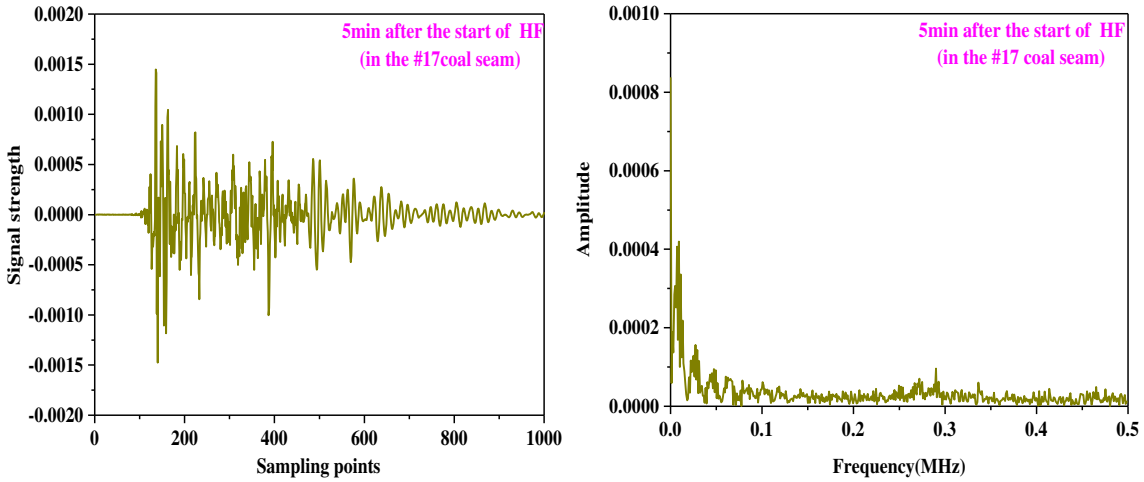

Fig. 8 Typical waveforms and frequency spectra of EMR signals 5 min after the start of HF

$$N_l = \int_0^{S_1} N_0 dS \tag{8}$$

The EMR pulse generated by the fracture of coal mass in S_2 is N_f:

$$N_f = \int_0^{S_2} N_0 dS, \tag{9}$$

It is obvious that:

$$N_l < N_f \tag{10}$$

That is why EMR signals are stronger when the jet flow impacts the coal mass in the **V** region compared with the coal mass in the **IV** region.

The relationship between EMR and gas pressure

Coal or rock undergoes volumetric expansion because of swelling stress when gas is adsorbed, and shrinkage when gas is desorbed; which is closely related to failure characteristics. There are many pores and fissures in coal or rock. Attractive forces exist in any two fissures, which can be broken by the absorption of gas. Swelling stress forms and dilatation energy is released, which can cause volumetric expansion. Surface physical chemistry studies have shown that when no gas exists between two fissures, the adsorption energy can be expressed by the following equation (Fu et al. 2002):

$$\mathrm{E} = \frac{1}{12\pi} \cdot \frac{H}{X^2} \tag{11}$$

where E is adsorption energy of a crack surface in a unit area; X is the distance between two fissures; H is the Hamaker constant. When gas is adsorbed on the fissures, adsorption energy will change, and the energy difference can be released as the dilatation energy. The dilatation energy is (Liu et al. 2010):

$$\Delta \mathrm{E} = \mathrm{E} - E' = \frac{1}{12\pi} \cdot \frac{\left(2\sqrt{H_1 H_2} - H_2\right)}{X^2} \tag{12}$$

The Hamaker constant is related to gas pressure, density, and polarizability for coal. The equation can be simplified as:

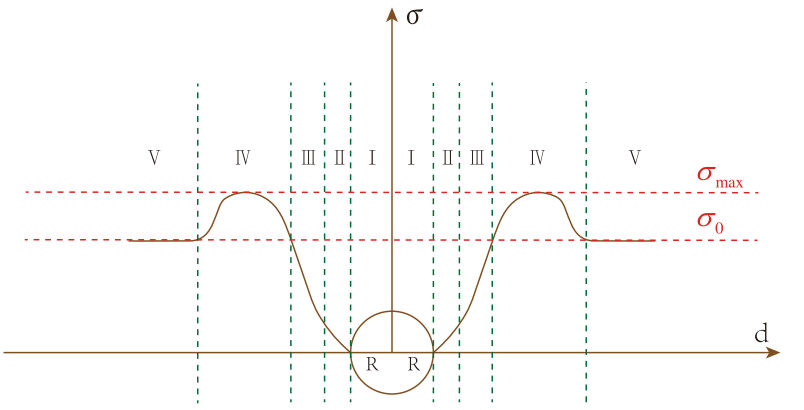

Fig. 9 Stress distribution of a borehole

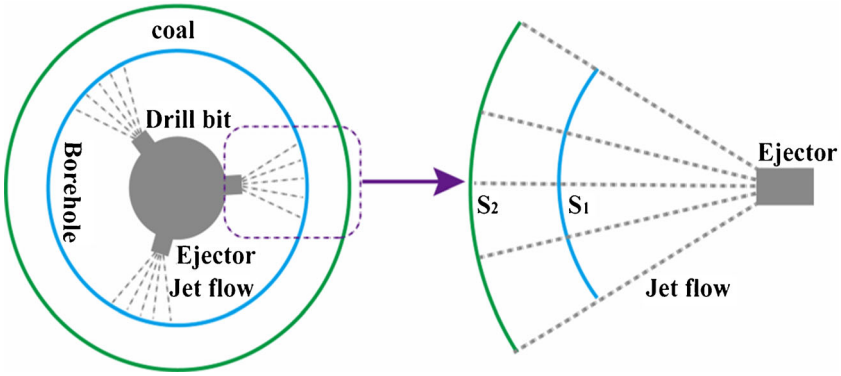

Fig. 10 Diagram of high-pressure water jet impacts on coal

$$\Delta E = \frac{K_1 - K_2 \alpha P}{X^2} \cdot \alpha \cdot P \tag{13}$$

where ΔE is the dilatation energy; P is the gas pressure in the pore; α is the polarizability of gas; and K_1 and K_2 are constants of coal.

The above Eq. (13) shows that dilatation energy has a quadratic function relationship with gas pressure, which means that dilatation energy increases with increasing gas pressure and coal failure will be more serious when gas desorbs under loading. So, the coal mass in the #18 coal seam with higher gas pressure will be broken more dramatically than that of the #17 coal seam under the same water pressure. Higher rupture velocity will be achieved if the failure of coal mass is more drastic. So, from the theory of brittle fracture mechanics, the rupture velocity can be obtained (Freund 1972):

$$V = \sqrt{\frac{2\pi E}{k\rho}}\left(1 - \frac{l_0}{l}\right) \tag{14}$$

where V is the rupture velocity; E is the elasticity modulus; ρ is the density of coal or rock; k is constant; l_0 is the initial length of the crack; l is the length of the extended crack. Taking the derivative of both sides with respect to time:

$$\frac{\partial V}{\partial t} = \sqrt{\frac{2\pi E}{k\rho}} \cdot \frac{l_0}{l^2} \cdot \frac{\partial l}{\partial t} = V \cdot \sqrt{\frac{2\pi E}{k\rho}} \cdot \frac{l_0}{l^2} = \frac{2\pi E}{k\rho} \cdot \frac{l_0}{l^2}\left(1 - \frac{l_0}{l}\right) \tag{15}$$

we obtain the accelerated velocity of crack extension. It is obvious that:

$$\frac{\partial V_{17}}{\partial t} < \frac{\partial V_{18}}{\partial t} \tag{16}$$

Electric double layer will be formed and change between fissures during coal fracturing, which can generate magnetic signals. The electric quadrupole of EMR under loading was analyzed and an expression of the electric field and magnetic field of the electric quadrupole by combining electrodynamics was obtained (Guo and Liu 1995).

$$E_N = \frac{3\mu_0}{2\pi} \cdot \frac{\partial V}{\partial t} \cdot \frac{p}{R^2} \sin\theta\cos\theta e_\varphi + \frac{\mu_0}{2\pi} \cdot \frac{\partial V}{\partial t} \cdot \frac{p}{R^2}\left(3\cos^2\theta - 1\right) e_R \tag{17}$$

$$B_N = \frac{3\mu_0}{2\pi} \cdot \frac{\partial V}{\partial t} \cdot \frac{p}{R^3} \sin\theta\cos\theta e_\varphi \tag{18}$$

It is obvious that E_N and B_N have a directly proportional relationship with $\frac{\partial V}{\partial t}$:

$$E_N \sim \frac{\partial V}{\partial t} \tag{19}$$

$$B_N \sim \frac{\partial V}{\partial t} \tag{20}$$

So from formulas (19) and (20), the following results are achieved:

$$E_{17} < E_{18} \tag{21}$$

$$B_{17} < B_{18} \tag{22}$$

These prove that EMR signals are stronger in the #18 coal seam than those in the #17 coal seam during HF.

In conclusion, before the start of HF, there were no EMR signals. At the beginning of HF, when the coal mass is impacted by the jet flow, EMR signals are weak. As HF continues, the action of the jet flow loaded on the surface of the coal mass increases. In the monitoring time, EMR signals will become stronger, which is proof that EMR signals increase with increasing time. When the hole is large enough, the jet flow is not strong enough to break coal any more, and the EMR signals decrease. After the end of HF, small EMR signals are generated by coal creep. The stronger the EMR signals, the better the effect of coal fracturing and the better the gas extraction after

the start of HF. We can judge the effect of coal failure by the EMR signals, which have a direct correlation with the efficiency of gas extraction.

Conclusions

EMR signals are generated during HF because of the fracture and deformation of coal caused by the high-pressure water jet. To further understand the process of coal failure during HF, the following conclusions were obtained by analyzing EMR signals:

1. The intensity of EMR signals at different times during HF was obviously different. EMR signals were positively associated with the degree of coal failure. Early in the HF process, increasing amounts of broken coal mass are ejected along the drill way and an increasingly larger hole is formed in the coal seam, which causes increasingly serious fractures and stronger EMR signals. At the end, EMR signal strength begins to decrease, which means that the hole in the coal seam is no longer growing. HF needs to stop when the EMR signals begin to decrease. At the same time, the count of EMR pulses can be used to analyze the rupture of coal. The higher the count of EMR pulses, the more serious the coal rupture. In the initial stage of HF, EMR pulses are relatively low. The highest EMR pulses are generated in the middle stage when large fractures occur. In the later stage, the higher EMR pulses began to disappear because of no serious ruptures.
2. When HF is conducted in different coal seams with different mechanical properties, the conditions of coal failure are different, resulting in different EMR signal intensities. The gas pressure of a coal seam directly influences EMR signal intensity. The greater the gas pressure in the coal seam, the more dilatation energy was released with the fracture of coal. Higher rupture velocity could generate stronger magnetic signals.
3. EMR frequencies that relate to coal deformation and fracture were obtained by converting the EMR signals from time domain to frequency with FFT. As HF continued, the principal frequencies and the amplitudes of waves increased gradually with gradually increasing ruptures. The principal frequencies and amplitudes were highest in the middle of HF because of the most serious fractures. These two indicators began to slowly decline in the later stages.

Acknowledgments We thank the anonymous reviewers for their comments and suggestions to improve the manuscript.

Funding information This work is supported by the "National natural science foundation of China (Grant No. 51574231)."

References

Bamberger L, Stieger J, Buchmann N, Eugster W (2014) Spatial variability of methane: attributing atmospheric concentrations to emissions. Environ Pollut 190:65–74. https://doi.org/10.1016/j.envpol.2014.03.028

Cao ZY, He XQ, Wang EY, Kong B (2018) Protection scope and gas extraction of the low-protective layer in a thin coal seam: lessons from the Dahe coalfield, China. Geosci J 22(3):487–499. https://doi.org/10.1007/s12303-017-0061-1

Chishko KA, Charkina OV (1997) Radiation of electromagnetic waves from edge dislocations moving in ionic crystal. Mater Sci Eng A234-236:361–364. https://doi.org/10.1016/S0921-5093(97)00134-2

Freund LB (1972) Crack propagation in an elastic solid subjected to general loading—II. Non-uniform rate of extension. J Mech Phys Solids 20:141–152. https://doi.org/10.1016/0022-5096(72)90007-5

Frid V (1997) Rockburst hazard forecast by electromagnetic radiation excited by rock fracture. Rock Mech Rock Eng 30(4):229–236. https://doi.org/10.1007/BF01045719

Fu XH, Qin Y, Jiang B, Wang WF (2002) Study on mechanics experiments of multiphase medium coal rocks. Geol J China Univ 4:446–452. https://doi.org/10.16108/j.issn1006-7493.2002.04.010 (in Chinese)

Geng JB, Xu J, Nie W, Peng SJ, Zhang CL, Luo XH (2017) Regression analysis of major parameters affecting the intensity of coal and gas outbursts in laboratory. Int J Min Sci Technol 27:327–332. https://doi.org/10.1016/j.ijmst.2017.01.004

Gonzatti C, Zorzi L, Agostini IM, Fiorentini JA, Viero AP, Philipp RP (2014) In situ strength of coal bed based on the size effect study on the uniaxial compressive strength. Int J Min Sci Technol 24(6):747–754. https://doi.org/10.1016/j.ijmst.2014.10.003

Guo ZQ, Liu B (1995) Frequency properties of electromagnetic emission associated with microscopic cracking in rocks. Chin J Geophys 38(2):221–226. https://doi.org/10.1016/0148-9062(96)89930-X Chinese Edition

He MC, Miao JL, Feng JL (2010) Rock burst process of limestone and its acoustic emission characteristics under true-triaxial unloading conditions. Int J Rock Mech Min Sci 47:286–298. https://doi.org/10.1016/j.ijrmms.2009.09.003

He XQ, Chen WX, Nie BS, Mitri H (2011) Electromagnetic emission theory and its application to dynamic phenomena in coal-rock. Int J Rock Mech Min Sci 48:1352–1358. https://doi.org/10.1016/j.ijrmms.2011.09.004

He XQ, Nie BS, Chen WX, Wang EY, Dou LM, Wang YH, Liu MJ, Mitri H (2012) Research progress on electromagnetic radiation in gas-containing coal and rock fracture and its applications. Saf Sci 50(4):728–735. https://doi.org/10.1016/j.ssci.2011.08.044

Kong B, Wang EY, Li ZH, Wang XR, Liu XF, Li N, Yang YL (2016a) Electromagnetic radiation characteristics and mechanical properties of deformed and fractured sandstone after high temperature treatment. Eng Geol 209:82–92. https://doi.org/10.1016/j.enggeo.2016.05.009

Kong XG, Wang EY, Liu XF, Li N, Chen L, Feng JJ, Kong B, Li DX, Liu QL (2016b) Coupled analysis about multi-factors to the effective influence radius of hydraulic flushing: application of response surface methodology. J Nat Gas Sci Eng 32:538–548. https://doi.org/10.1016/j.jngse.2016.04.043

Kong B, Wang EY, Li ZH, Niu Y (2017) Time-varying characteristics of electromagnetic radiation during the coal-heating process. Int J Heat Mass Transf 108:434–442. https://doi.org/10.1016/j.ijheatmasstransfer.2016.12.043

Lichtenberger M (2006) Underground measurements of electromagnetic radiation related to stress-induced fractures in the Odenwald

mountains. Pure Appl Geophys 163(8):1661–1677. https://doi.org/10.1007/s00024-006-0083-5

Liu JZ (2009) The control of coal mine gas and coordinated exploitation of coal bed methane in China. J Coal Sci Eng 15(3):267–272. https://doi.org/10.1007/s12404-009-0310-7

Liu HB, Cheng YP (2015) The elimination of coal and gas outburst disasters by long distance lower protective seam mining combined with stress-relief gas extraction in the Huaibei coal mine area. J Nat Gas Sci Eng 27:346–353. https://doi.org/10.1016/j.jngse.2015.08.068

Liu YB, Cao SG, Li Y, Wang J, Guo Q, Xu J, Bai YJ (2010) Experimental study of swelling deformation effect of coal induced by gas adsorption. Chin J Rock Mech Eng 12:2484–2491. https://doi.org/10.16108/j.issn1006-7493.2002.04.010 (in Chinese)

Liu XF, Wang XR, Wang EY, Kong XG, Zhang C, Liu SJ, Zhao EL (2017) Effects of gas pressure on bursting liability of coal under uniaxial conditions. Journal of Natural Gas Science and Engineering 39:90–100. https://doi.org/10.1016/j.jngse.2017.01.033

Lou Q, Song DZ, He XQ, Li ZL, Qiu LM, Wei MH, He SQ (2019) Correlations between acoustic and electromagnetic emissions and stress drop induced by burst-prone coal and rock fracture. Saf Sci 115:310–319. https://doi.org/10.1016/j.ssci.2019.02.022

Nie BS, He XQ, Wei ZC (2009) Study on mechanical property and electromagnetic emission during the fracture process of combined coal-rock. Procedia Earth Planet Sci 1(1):281–287. https://doi.org/10.1016/j.proeps.2009.09.045

Nitsan U (1977) Electromagnetic emission accompanying fracture of quartz-bearing rocks. Geophys Res Lett 15(4):333–336. https://doi.org/10.1016/0148-9062(78)91244-5

Pan YS (2016) Integrated study on compound dynamic disaster of coal-gas outburst and rockburst. J China Coal Soc 41(1):105–112. https://doi.org/10.13225/j.cnki.jccs.2015.9034 (in Chinese)

Qiu LM, Wang EY, Song DZ (2017) Measurement of the stress field of a tunnel through its rock EMR. J Geophys Eng 14:949–959. https://doi.org/10.1088/1742-2140/aa6dde

Shen RX, Qiu LM, Lv GG, Wang EY, Li HR, Han X, Zhang X, Hou Z (2018) An effect evaluation method of coal seam hydraulic flushing by EMR. Journal of Natural Gas Science and Engineering 54:154–162. https://doi.org/10.1016/j.jngse.2018.03.030

Shen RX, Qiu LM, Zhao EL, Han X, Li HR, Hou ZH, Zhang X (2019) Experimental study on frequency and amplitude characteristics of acoustic emission during the fracturing process of coal under the action of water. Saf Sci 117:320–329. https://doi.org/10.1016/j.ssci.2019.04.031

Song DZ, Wang EY, Li ZH, Liu J, Xu WQ (2015) Energy dissipation of coal and rock during damage and failure process based on EMR. Int J Min Sci Technol 25(5):17–30. https://doi.org/10.1016/j.ijmst.2015.07.014

Song DZ, Wang EY, Song XY, Jin PJ, Qiu LM (2016) Changes in frequency of electromagnetic radiation from loaded coal rock. Rock Mech Rock Eng 49:291–302. https://doi.org/10.1007/s00603-015-0738-6

Wang EY, Zhao EL (2013) Numerical simulation of electromagnetic radiation caused by coal/rock deformation and failure. Int J Rock Mech Min Sci 57:57–63. https://doi.org/10.1016/j.ijrmms.2012.07.002

Wang EY, He XQ, Liu XF, Li ZH, Wang C, Xiao D (2011) A non-contact mine pressure evaluation method by electromagnetic radiation. J Appl Geophys 75(2):338–344. https://doi.org/10.1016/j.jappgeo.2011.06.028

Wang XX, Shi BM, Mu CM (2012a) Study on formation mechanism of gas partition in hydraulic flushing coal seam. J China Coal Soc 37(3):467–471. https://doi.org/10.13225/j.cnki.jccs.2012.03.028 (in Chinese)

Wang C, Xu JK, Zhao XX, Wei MY (2012b) Fractal characteristics and its application in electromagnetic radiation signals during fracturing of coal or rock. Int J Min Sci Technol 22(2):255–258. https://doi.org/10.1016/j.ijmst.2012.03.003

Wang L, Cheng LB, Cheng YP, Yin GZ, Xu C, Jin K, Yang QL (2014) Characteristics and evolutions of gas dynamic disaster under igneous intrusions and its control technologies. Journal of Natural Gas Science and Engineering 18:164–174. https://doi.org/10.1016/j.jngse.2014.02.012

Xie SR, Li EP, Li SJ, Wang JG, He CC, Yang YF (2015) Surrounding rock control mechanism of deep coal roadways and its application. Int J Min Sci Technol 25(3):429–434. https://doi.org/10.1016/j.ijmst.2015.03.016

Yang YF, Wang NH (2010) Analysis on pressure releasing and permeability improving technology with hydraulic borehole jetting in Yian mine. Coal Sci Technol 38(7):48–51. https://doi.org/10.13199/j.cst.2010.07.56.yangyf.028 (in Chinese)

Zhou FB, Sun YL, Li HJ, Yu GF (2016) Research on the theoretical model and engineering technology of the coal seam gas drainage hole sealing. J China Univ Min Technol 45(3):433–439. https://doi.org/10.13247/j.cnki.jcumt.000498 (in Chinese)